International Core Journal of Engineering Volume 11 Issue 4, 2025
ISSN: 2414-1895 DOI: 10.6919/ICJE.202504_11(4).0024

# Effect of Oxidation Voltage on Micro-Arc Oxide Film of CNT/2024 Aluminum Matrix Composites

Lei Zhou

School of Materials and Chemistry, University of Shanghai for Science and Technology, Shanghai 200093, China

## Abstract

**CNT/2024 AMCs (aluminum matrix composites) have great application prospects in the aerospace field due to their excellent mechanical properties. In order to enhance the corrosion resistance of the material, a micro-arc oxidation process was used to form an oxide ceramic layer on the surface of the material, and the effect of oxidation voltage on the morphology and properties of the film was investigated. With the increase of voltage, the number of micropores on the surface of the oxide layer decreased, the pore size increased, and the thickness gradually increased. When the voltage reached 430 V, cracks appeared on the surface of the oxide layer. When the voltage was 470 V, a new α-Al2O3 diffraction peak was generated at about 63.5° due to the excessive energy density on the surface of the sample. In the voltage range of 350 V to 430 V, the hardness and corrosion resistance of the oxide layer are positively correlated with the voltage, but when the voltage reaches 470 V, the hardness and corrosion resistance decrease due to the large pore size.**

## Keywords

**CNT/2024 AMCs; Microarc Oxidation; Oxidation Voltage; Hardness; Corrosion.**

## 1. Introduction

Aluminum is the third most abundant element in the crust (about 8.23%), and its mineral resources are second only to oxygen and silicon. Although aluminum has the advantage of reserves and is widely used in various industrial fields, its own characteristics still have significant application limitations. First of all, in the natural environment, aluminum is easy to combine with oxygen to form a dense oxide film, resulting in the natural aluminum mainly in bauxite, feldspar ($KAlSi_3O_8$) and other compounds. Secondly, the ultimate tensile strength of pure aluminum is only about 90 MPa, which is difficult to meet the high strength needs of modern industry for structural materials. For this reason, aluminum alloy materials with significantly improved mechanical properties have been developed by alloying technology. In recent years, it has been further found that Aluminum Matrix Composites (AMCs) constructed by introducing reinforced phases can break through the performance bottleneck of traditional alloys[1,2]. As a typical multiphase system, the macroscopic performance of AMCs depends on the synergistic mechanism between matrix and reinforcement, which involves four key structural elements: metal matrix, reinforcement phase, intermediate transition layer and interface binding zone. Compared with the traditional aluminum alloy, the composite modified material shows a variety of performance advantages: high strength-weight ratio and high specific modulus; Excellent high temperature stability and creep resistance; Significantly improved wear resistance and fatigue resistance; Low coefficient of thermal expansion and good damping performance[3]. More importantly, by adjusting the type of reinforcement phase (such as SiC, $Al_2O_3$, graphite, etc.), volume fraction and spatial distribution parameters, the gradient design and function customization of

ISSN: 2414-1895 DOI: 10.6919/ICJE.202504_11(4).0024

material properties can be realized, and this designability feature makes it one of the most adaptable systems in the metal matrix composite family.

Although the mechanical properties of aluminum matrix composites are significantly improved by heterogeneous composites, their poor corrosion resistance often becomes a shortcoming restricting engineering applications[4]. Studies have shown that the introduction of the reinforcing phase breaks the electrochemical homogeneity of the material system, especially in the medium containing Cl, the microcouple formed between the high-potential enhancer such as carbon nanotubes and SiC and the aluminum matrix will cause a significant potential difference, resulting in the preferential dissolution of the matrix[5]. Taking the carbon nanotube reinforcement system as an example, the metastable $Al_4C_3$ phase is easily formed at the interface during the high temperature preparation process, and the phase is prone to hydrolysis in a humid environment and accompanied by volume changes. The resulting interfacial microcracks become the preferred path for the penetration of corrosive media. In addition, the high-density dislocation region formed by the mismatch of thermal expansion coefficient around the reinforcement further intensifies the electrochemical activity of the material surface. It is worth noting that when a semiconductor-type reinforcement phase is used, photogenerated carrier migration may be induced under a specific wavelength of light. This photoelectric coupling effect dynamically modulates the interfacial charge distribution, making the material exhibit the dual corrosion characteristics of photoinduced corrosion acceleration or cathodic protection[6]. In order to meet the above challenges, surface modification technologies such as micro-arc oxidation and electroless plating are generally used in engineering practice to block the corrosion reaction path by constructing a dense passivation layer or a sacrificial protective layer, thereby effectively prolonging the service life of the material in harsh environments.

Micro-arc oxidation (MAO), also known as plasma electrolytic oxidation (PEO), is a surface treatment process in which a high-voltage electric field is applied to lightweight alloy materials such as aluminum, magnesium, and titanium in a specific electrolytic medium, and a dense oxide ceramic coating is finally generated on the surface of the workpiece by using the thermo-electric-plasma multi-field coupling effect[7,8]. The specific process is as follows: the initial formation of a sub-micron anodic oxide film on the surface of the substrate, and the plasma spark phenomenon occurs on the surface with the increase of the applied voltage layer. The oxide coating that meets the preset film thickness requirements is finally obtained by continuous micro-discharge electrocoagulation. Compared with traditional anodic oxidation, this process relies on high-voltage electric environment to achieve film growth, and the workpiece is maintained in the high-potential domain throughout the process, which is significantly different from the Faraday reaction zone of conventional anodic oxidation.

The setting of oxidation voltage plays an important role in regulating the microstructure and function of micro-arc oxidation ceramic coatings[9]. The results show that the ion migration rate and plasma discharge intensity change significantly when the voltage gradient changes in the range of 200-400 V. When the applied voltage is lower than 160 V, the strong field effect of oxidation reaction is obviously insufficient, resulting in the coating deposition rate lower than 0.8 μm/min, and the generated γ-$Al_2O_3$ phase content is higher. When the voltage exceeds the critical value of 450 V, the discharge energy density per unit area will rise to 12 kJ/cm$^2$, which will lead to two negative effects - one is that the average pore diameter of the micropore expands from 4-6 μm to more than 10 μm, and the other is that the surface stress crack density increases by about 75% through microhardness test[10,11]. In view of the dynamic law of voltage parameters and film thickness changes, Liu Junchao et al. revealed the evolution characteristics of three stages through the real-time volt-thickness monitoring system: in the initial film forming stage (0-10 min), the voltage stabilized at 280±20 V stage, at which time the film thickness increased linearly at a rate of 2.3 μm/min; During the transition period (10-25 min), the voltage gradient increased to 350 V, the cooling rate of the melt in the electrolyte increased to 106 K/s, and the densification rate decreased to 1.1 μm/min. In the stable period (after 25 min), the voltage fluctuation amplitude exceeds ± 15%, and the microstructure characterization shows that the dense layer/loose layer thickness ratio decreases from the initial 3:1

ISSN: 2414-1895 DOI: 10.6919/ICJE.202504_11(4).0024

to 1.8:1, and the surface Vickers hardness value should be reduced from 1350 HV to 950 HV. Therefore, the selection of suitable oxidation voltage plays an important role in the preparation of micro-arc oxide film.

The research focus of this paper is to improve the corrosion resistance of CNT/2024Al. By adjusting the oxidation voltage, the suitable voltage parameters for CNT/2024 ACM materials are found, which provides a reference for the preparation of micro-arc oxide films of aluminum matrix composites with reinforced phases such as carbon nanotubes.

## 2. Material and Methods

### 2.1 Experimental Materials and Pretreatment

In this paper, we studied CNT/2024 aluminium extrusion composites prepared based on elemental alloying and hot extrusion process, in which the volume percentage of carbon nanotubes was 1.32%. The CNT/2024 aluminium matrix composite substrate was cut into Φ12 mm×2 mm circular samples. After that, it was sequentially sanded with 400, 800, 1500 and 2000 - mesh silicon carbide sandpaper, followed by ultrasonic cleaning with acetone.

### 2.2 Selection of Electrical Parameters and Electrolyte Configuration

The micro-arc oxidation equipment used in this test is the MAO30HD-III micro-arc oxidation power supply. The power supply mode is constant voltage mode and the voltage is selected as 350 V, 390V, 430V and 470V. The oxidation time was 6 min, the frequency was 500 Hz, and the duty cycle was 20%. The electrolyte is set to 15 g/L $Na_2SiO_3$ and 2 g/L NaOH.

### 2.3 Characterization of MAO Coating

A QUANTA FEG 450 field emission ambient SEM was utilized to observe the surface and cross-section topography of the MAO films. A D8 ADVANCE model XRD was used to characterise the surface phases of the MAO films. The coating corrosion endurance measurements were conducted using an electrochemical workstation, model CHI760E, manufactured by Shanghai Chenhua Co. Ltd.

## 3. Results and Discussion

### 3.1 Surface Morphology of MAO Coatings

FIG. 1 is the SEM diagram of the oxide layer under different oxidation voltages. It can be seen from the diagram that volcanic type holes are generated under each voltage, and the number of holes gradually decreases with the increase of voltage, while the pore size gradually increases. When the oxidation voltage is 350 V, the micropore diameter is small and the surface is flat, there is no melt-like protrusion, and there is no crack on the surface of the oxide layer, but it can be found that part of the oxide layer is stripped. This is because the coating growth rate is slow at low voltage and the thickness is thin, the discharge spark can easily penetrate the oxide layer, and a large number of holes can be generated. However, due to the low intensity of micro-arc discharge at low voltage, the microhole aperture is small. The partial peeling phenomenon is due to the impact of bubbles when the molten oxide is not completely solidified during the formation of the oxide layer, so that the affected part is not covered on the surface to form a peeling phenomenon. When the voltage increases to 390 V, the number of micropores decreases, the pore size increases, and the distribution of micropores is less uniform, but no obvious cracks appear. Due to the thin oxide layer, scratches left by grinding can be seen on the surface. With the increase of voltage, the mass of molten oxide produced is larger, and it is not susceptible to bubble impact, so no stripping phenomenon of oxide layer is found on the surface. When the voltage is increased to 430 V, the number of microholes is further reduced and the aperture is increased. Fine cracks and granular melts appear on the surface of the oxide layer, and the generation of cracks is related to the thermal stress gradient density generated by the solidification process when the molten oxide is in contact with the cold electrolyte. The increase in the thickness of the oxide layer will generate higher residual stress, promote the formation and expansion of micro-cracks, and the surface of the oxide layer will become rougher [12]. When

ISSN: 2414-1895 DOI: 10.6919/ICJE.202504_11(4).0024

the voltage is further increased to 470 V, the high voltage will cause the micro-arc discharge phenomenon to be more intense, and the instantaneous energy generated is higher. The high intensity discharge will form large spark discharge spots on the surface, resulting in a large discharge channel, resulting in the increase of micropore diameter.

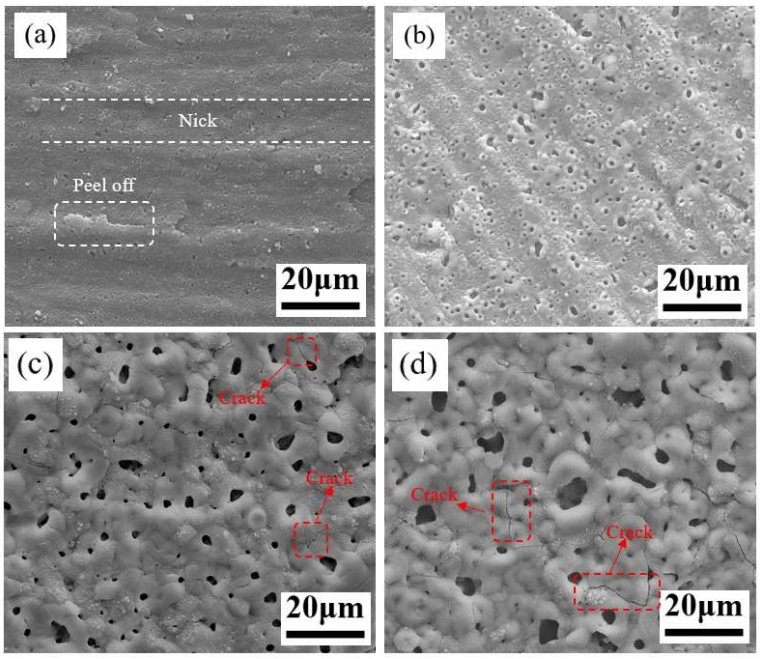


**Figure 1.** Micromorphology of oxide layer under different oxidation voltages: (a) 350 V; (b) 390 V; (c) 430 V; (d) 470 V

### 3.2 Phase Composition Analysis of Oxide Layer

Figure 2 shows the XRD pattern of the oxide layer obtained at different oxidation voltages. It can be seen from the figure that the oxide layer obtained at different voltages is composed of α-$Al_2O_3$ and γ-$Al_2O_3$. With the increase of voltage, the diffraction peak of γ-$Al_2O_3$ increases slightly. At a voltage of 350 V, the XRD pattern has no significant difference compared with the substrate because the oxide layer is thin and can be easily penetrated by X-rays. With the increase of voltage, the peak of α- $Al_2O_3$ is more obvious, because α-$Al_2O_3$ is a high temperature transition phase, and the increase of temperature will cause γ-$Al_2O_3$ to transform into α-$Al_2O_3$[13]. At 470 V, new α- $Al_2O_3$ is produced at about 63.5 ° due to the increase of energy input.

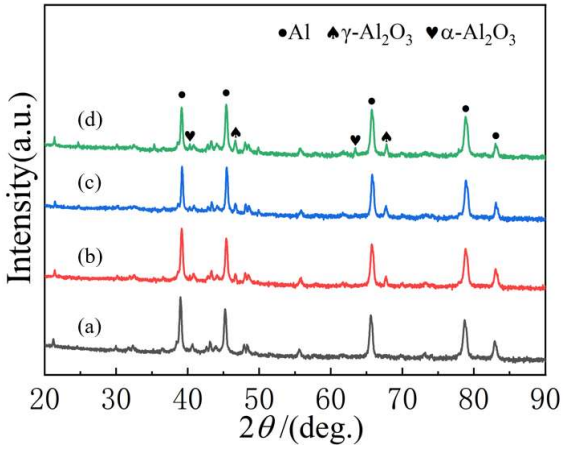


**Figure 2.** XRD patterns of oxide layers at different oxidation voltages (a) 350V, (b) 390V, (c) 430V, (d) 470V

ISSN: 2414-1895 DOI: 10.6919/ICJE.202504_11(4).0024

### 3.3 Morphology Analysis of Oxide Layer Cross Section

The cross section morphologies of oxide films obtained under different voltages are shown in Figure 3. As can be seen from the figure, the oxide layer thickness gradually increases with the increase of voltage. When the voltage is 350 V, the oxide layer thickness is the thinnest, which is 4.4 μm, and when the voltage reaches 470 V, the oxide layer thickness is the thickest, which is 10.7 μm. It can also be seen from the figure that when the voltage is low, the inner and outer layers of the oxide film are uneven, and there is a trend of inward and outward growth, but the oxide film has fewer defects and the coating is relatively dense. At high voltage, the inside and outside of the oxide film are relatively smooth, but there are more defects in the inside, and the higher the voltage, the more defects. This is because the growth rate of the oxide layer is slow and the thickness is thin at low pressure. When the micro-arc oxidation reaches the set time, the oxide layer still maintains the trend of inward and outward growth. With the increase of voltage, the growth rate of the oxide layer gradually increases, but too high voltage may cause part of the surface of the oxide layer to burn off. Due to excessive energy, the number of discharge channels increases, and the aperture increases, the internal defects of the oxide layer increase, and the structure gradually becomes loose.

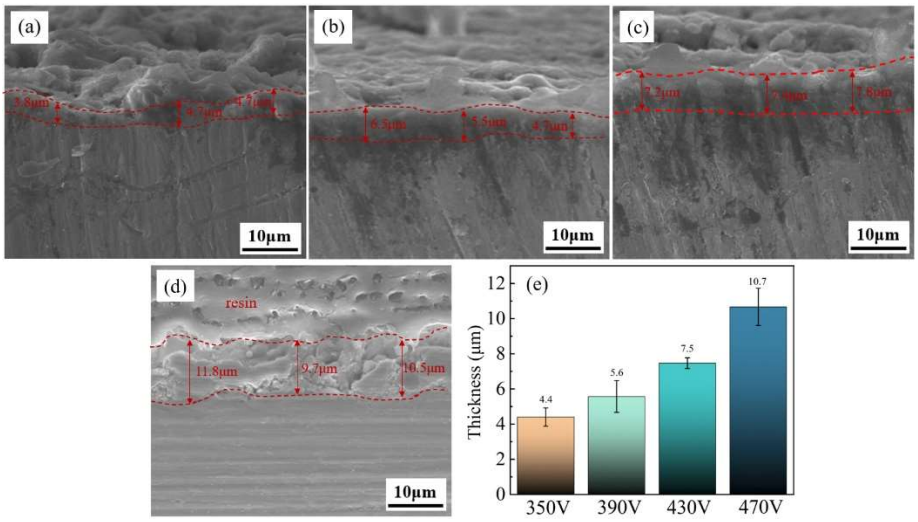


**Figure 3.** Morphology and thickness of oxide layer under different oxidation voltages: (a) 350 V; (b) 390 V; (c) 430 V; (d) 470 V; (e) Average oxide film thickness of each sample

### 3.4 Hardness Analysis of Oxide Layer

The variation law of oxide hardness under different voltages can be seen from Figure 4. As the oxidation voltage increases, the hardness of oxide layer increases. When the voltage increases to 430 V, the average hardness of the oxide layer reaches 483 HV, but when the voltage further increases to 470 V, the average hardness of the oxide layer decreases to 424 HV, which is caused by the excessive voltage and the rapid growth rate of the oxide layer.

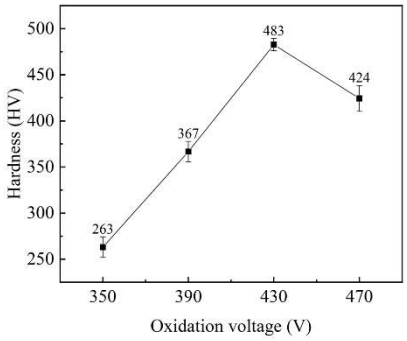


**Figure 4.** Hardness variation diagram of oxide layer under different oxidation voltages

ISSN: 2414-1895 DOI: 10.6919/ICJE.202504_11(4).0024

### 3.5 Analysis of Corrosion Resistance of Oxide Layer

The polarization curves of oxidation layer obtained under different oxidation voltages are shown in Figure 5. The polarization curves of samples with different oxidation layers are also fitted by extrapolation method to obtain corresponding corrosion potential and corrosion current density. The fitting results are shown in Table 3.5. As can be seen from the figure and table, with the increase of oxidation voltage in the range of 350 V to 430 V, the self-corrosion potential also gradually increases, from -0.48 V to -0.30 V, and the corrosion current density gradually decreases, from $1.66*10^{-6}$ A·cm$^2$ to $3.02*10^{-7}$ A·cm$^2$. This indicates that the corrosion resistance of the oxide layer is improved with the increase of the voltage, but the corrosion resistance is decreased when the voltage is increased to 470 V, which is because the excessive voltage leads to the increase of the surface aperture of the oxide layer, the film structure is more loose, and the corrosion liquid is easier to enter the film, resulting in the decline of the corrosion resistance.

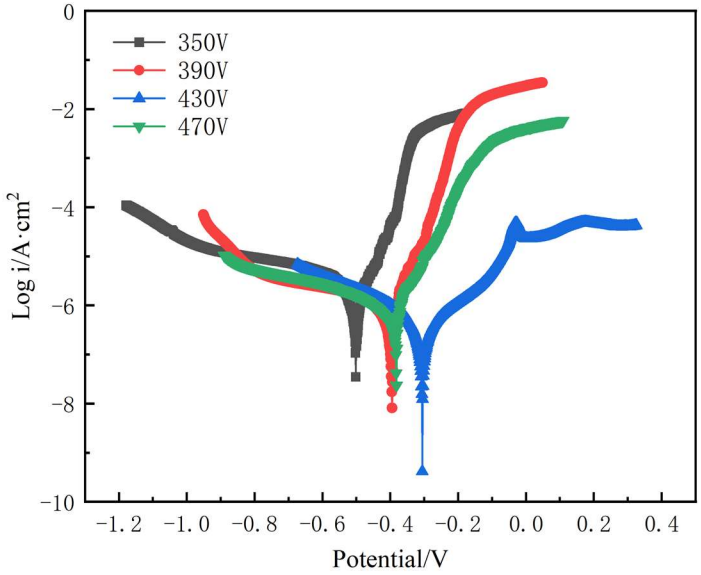


**Figure 5.** Polarization curves of oxide layer under different oxidation voltages

**Table 1.** Self-corrosion potential and self-corrosion current of oxide layer under different oxidation voltages

| Oxidation voltage(V) | 350 | 390 | 430 | 470 |
|---|---|---|---|---|
| Ecorr(V) | -0.48 | -0.42 | -0.30 | -0.39 |
| Icorr(A/cm$^2$) | $1.66*10^{-6}$ | $7.15*10^{-7}$ | $3.02*10^{-7}$ | $4.92*10^{-7}$ |

The Nyquist graph of the oxide layer prepared at different oxidation voltages is shown in Figure 6. From the figure, the capacitive reactance arc diameter at different voltages can be obtained: 430 V > 470 V > 390 V > 350 V. Equivalent circuit fitting is performed on the EIS data, and the fitting results are shown in the table. As can be seen from the table, the changes in the values of $R_1$ and $R_2$ at different voltages are consistent with the laws of the impedance arc. Among them, the values of $R_1$ and $R_2$ at 430 V are the highest, $1.03*10^4$ Ω·cm$^2$ and $1.26*10^5$ Ω·cm$^2$ respectively. Compared with $3.71*10^3$ Ω·cm$^2$ and $1.39*10^4$ Ω·cm$^2$ at 350V, the corrosion resistance of the oxide layer is the best, which is consistent with the results reflected by the potentiodynamic polarization curve.

ISSN: 2414-1895 DOI: 10.6919/ICJE.202504_11(4).0024

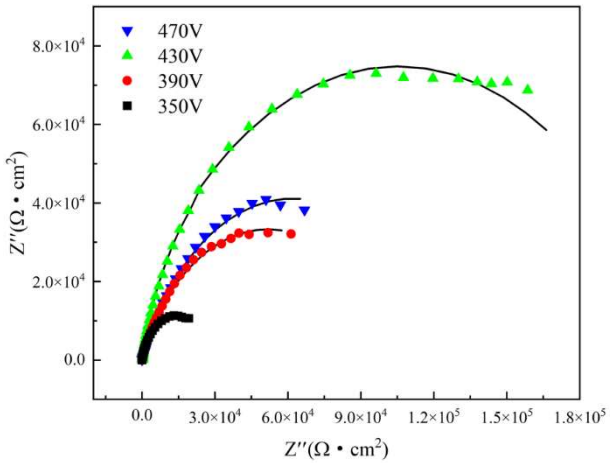


**Figure 6.** Nyquist curves at different oxidation voltages

**Table 2.** Parameters after equivalent circuit fitting of EIS curves for different oxidation voltages

| Samples | Rs ($\Omega \cdot cm^2$) | $CPE_1$ ($F \cdot cm^2$) | $n_1$ | $R_1$ ($\Omega \cdot cm^2$) | $CPE_2$ ($F \cdot cm^2$) | $n_2$ | $R_2$ ($\Omega \cdot cm^2$) |
|---|---|---|---|---|---|---|---|
| 350 V | 33.21 | $1.91*10^{-5}$ | 0.86 | $3.71*10^3$ | $1.84*10^{-5}$ | 0.87 | $1.39*10^4$ |
| 390 V | 42.56 | $2.61*10^{-5}$ | 0.71 | $5.16*10^3$ | $8.45*10^{-5}$ | 0.70 | $6.88*10^4$ |
| 430 V | 38.12 | $1.53*10^{-6}$ | 0.56 | $1.03*10^4$ | $7.34*10^{-6}$ | 0.73 | $1.26*10^5$ |
| 470 V | 30.22 | $4.84*10^{-6}$ | 0.52 | $6.98*10^3$ | $5.01*10^{-6}$ | 0.58 | $8.34*10^4$ |

## 4. Conclusion

Under the oxidation voltage gradient, the number of CNT/2024Al coating holes decreases with the increase of voltage, but the pore size increases. When the voltage is greater than 430 V, cracks appear on the surface. When the voltage is between 350 V and 430 V, the hardness and corrosion resistance of the oxide layer are proportional to the voltage, and the voltage is too large, which leads to the decline of the hardness and corrosion resistance of the coating. At 430 V, the hardness reaches the maximum of 483 HV, and the self-corrosion current density and impedance value also reach the maximum, which are $3.02*10^{-7}$ $A \cdot cm^2$ and $1.26*10^5$ $\Omega \cdot cm^2$, respectively. Therefore, the MAO coating has the best performance when the oxidation voltage is 430 V.

## References

[1] Y. Guangliang, L. Xianyi, B. Yizhen, C. Haifeng and J. Zengsun, The Effects of Current Density on the Phase Composition and Microstructure Properties of Micro-Arc Oxidation Coating, J. Alloys Compd., 2002, 345(1–2), p 196–200.

[2] Hong SK, Li QN, Qu JJ, Huang L, Zhao LB. Effects of Ce(NO3)3 additive on the properties of micro-arc oxidation coatings formed on 7075 aluminum alloy. China Surf Eng. 2014; 27(6):116.

[3] Li J, Zhou J, Feng A, et al. Analysis of microstructure and tensile properties produced by cryogenic laser peening on 2024-T351 aluminum alloy[J]. Vacuum, 2018, 158: 141-145.

[4] J.H. Wang, M.H. Du, F.Z. Han and J. Yang, Effects of the Ratio of Anodic and Cathodic Currents on the Characteristics of Micro-Arc Oxidation Ceramic Coatings on Al Alloys, Appl. Surf. Sci., 2014, 292, p 658–664.

[5] Sun QQ, Sun RJ, Chen SY, Chen QY, Chen KH. Effect of atmospheric pollutants on electrochemical corrosion behavior of 7B50 aluminium alloy. Chin J Nonferrous Met. 2015;25(3):575.

ISSN: 2414-1895 DOI: 10.6919/ICJE.202504_11(4).0024

[6] Zhang X, Zhao N, He C. The superior mechanical and physical properties of nanocarbon reinforced bulk composites achieved by architecture design – A review[J]. Progress in Materials Science, 2020, 113: 100672.

[7] Babak Haghighat Shishavan, Rasoul Azari Khosrowshahi, Safa Haghighat Shishavan, et al. Improving wear and corrosion properties of alumina coating on AA7075 aluminum by plasma electrolytic oxidation: Effects of graphite absorption[J]. Applied Surface Science, 2019, 481: 108-119.

[8] Gaoqiang Xu, Xingkun Shen. Fabrication of SiO2 nanoparticles incorporated coating onto titanium substrates by the micro arc oxidation to improve the wear resistance[J]. Surface and Coatings Technology, 2019, 364: 180-186.

[9] Yan H , Liu W , Yu Z ,et al.Effect of Sodium Tungstate on the Microstructure and Properties of Micro-Arc Oxidized Coatings Formed on 2A12 Aluminum Alloy[J].Journal of Materials Engineering and Performance, 2021(1–2).

[10] Aliramezani R, Raeissi K, Santamaria M, et al. Characterization and properties of PEO coatings on 7075 Al alloy grown in alkaline silicate electrolyte containing KMnO4 additive[J]. Surface and Coatings Technology, 2017, 329: 250-261.

[11] Echeverry-Rendon M, Duque V, Quintero D, et al. Improved corrosion resistance of commercially pure magnesium after its modification by plasma electrolytic oxidation with organic additives[J]. Journal of biomaterials applications, 2018, 33(5): 725-740.

[12] Wu X, Li H, Lu J, et al. MoS2 additive to the MAO Al2O3 composite coatings with enhanced mechanical performances[J]. Materials Research Express, 2018, 6(1): 016543.

[13] Zhang G, Wu L, Tang A, et al. Effect of micro-arc oxidation coatings formed at different voltages on the in situ growth of layered double hydroxides and their corrosion protection[J]. Journal of The Electrochemical Society, 2018, 165(7): C317.